# Ultra-Broad-Band Doubly Balanced Star Mixers Using Planar Mouw's Hybrid Junction

Chi-Yang Chang, *Member, IEEE,* Ching-Wen Tang, and Dow-Chih Niu

***Abstract*—Ultra-broad-band star mixers using planar Mouw's hybrid junction [1] are presented in this paper. The planar Mouw's hybrid junction is realized by coplanar waveguide (CPW) to coplanar strip (CPS) or CPW to CPW T-junctions. A new explanation of Mouw's theory based on coupled transmission lines and including the transmission line losses is presented. The modified theory is more suitable for ultra-broad-band mixer design. Some prototype mixers with CPW to CPS or CPW to CPW T-junctions are fabricated with $Al_2O_3$ substrate. The prototype mixers show a bandwidth of greater than 20 : 1 if the even-mode resonance has been damped out. Method for damping out the even-mode resonance is also presented. All of the prototype circuits show much broader bandwidth than that of conventional star mixer.**

***Index Terms*—Doubly balanced mixer, hybrid junction, star mixer, ultra-broad-band mixer.**

## I. Introduction

ULTRA-BROAD-BAND, typically greater than 10 : 1 bandwidth, microwave mixers are an important component in the applications such as instrumentation, electronic warfare (EW), electronic support measures (ESMs), electronic counter measures (ECMs), and electronic counter-counter measures (ECCMs), etc. For example, a mixer for instrument application is common to cover a frequency of 1–18 GHz or even to 26.5 GHz. The most popular ultra-broad-band mixer is a ring-type doubly balanced mixer. A ring-type doubly balanced mixer uses two single baluns for RF and local oscillator (LO) ports, and is usually realized by a soft-board and three-dimensional (3-D) structure. The star mixer is an alternative doubly balanced configuration. There are many advantages of the star mixer comparing to that of a ring mixer. One of them is that the IF/RF or IF/LO diplexing circuit, which is essential in most ring mixers, is eliminated. The IF signal can be directly picked out from center of the star diode quad. However, the reported star mixers do not show ultra-broad-band performance.

Two dual baluns are required to feed the balanced signals to the diode quad in a star mixer. The conventional star mixer [2]–[4] uses a modified Marchand-type dual balun [5]. A coaxial line, 3-D parallel-plate transmission line, coplanar waveguide (CPW), or microstrip can realize the Marchand-type dual balun. A pair of perpendicularly oriented Marchand-type dual baluns [2]–[4] can realize a conventional star mixer. The diode quad is placed at the center of two dual baluns. The bandwidth of a conventional star mixer, typically 2 : 1 bandwidth, is mainly limited by this Marchand-type dual balun. When performing the ultra-broad-band measurement, the conventional star mixer periodically shows passband and stopband. The stopbands of the conventional Marchand-type star mixer are very wide and cannot be eliminated by the method proposed in this paper because the stopbands of the conventional star mixer are not caused by the resonant phenomenon as the proposed Mouw's star mixer does.

In this paper, we propose a star mixer using a planar Mouw's hybrid junction [1], which can achieve ultra-broad-band performance. The theory of original Mouw's hybrid junction cannot realize an ultra-broad-band mixer because the theory in Mouw's paper is based on lossless transmission lines. As the transmission line loss is introduced into the hybrid junction properly, this newly proposed star mixer could be an ultra-broad-band mixer. The hybrid junction proposed by Mouw [1] comprises a pair of perpendicularly placed T-junctions. A single T-junction may be considered as a dual balun. The bandwidth of a single T-junction dual balun is unlimited as long as the impedance is matched. However, when the second T-junction dual balun is connected to form a Mouw's hybrid junction, the even-mode resonance, as will be explained in the following section, occurs periodically. Theoretically, this resonant phenomenon causes conversion loss dips near the resonant frequencies. The Mouw's star mixer also shows multiple numbers of passbands and stopbands due to this resonant phenomenon. According to the theory in the following section, the stopbands can be quite narrow if the even-mode characteristic impedance is much higher than the odd-mode characteristic impedance. Therefore, the stopbands (the resonant dips) can be removed by increasing the damping factor of the resonance. An effective method to damp out the resonance is proposed in this paper.

The suspended substrate coplanar strips (SSCPSs), the conductor-backed coplanar strips (CBCPSs), and the absorber-backed coplanar strips (ABCPSs) are three proposed transmission-line structures to realize a Mouw's star mixer and to compare their ultra-broad-band performance. The conversion loss dips can be found in the Mouw's mixers realized by SSCPSs or CBCPSs. The Mouw's mixers realized by ABCPSs, however, show very good ultra-broad-band performance because the absorber damps the resonant dips out. The theoretical analysis for damping out the resonant dips is discussed in the following section.

Manuscript received August 4, 2000. This work was supported in part by the Ministry of Education under Grant 89-E-FA06-2-4.

C.-Y. Chang and C.-W. Tang are with the Department of Communication Engineering, National Chiao Tung University, Hsinchu, Taiwan, R.O.C.

D.-C. Niu is with the Chung-Shan Institute of Science and Technology, Lung-Tang, Taiwan, R.O.C.

Publisher Item Identifier S 0018-9480(01)03998-9.

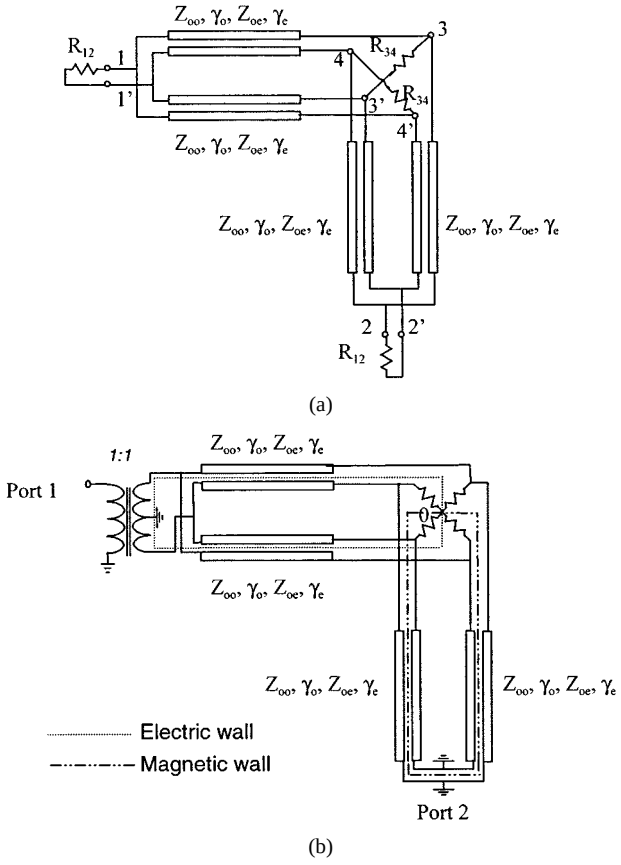


Fig. 1. (a) Mouw's hybrid junction with each transmission lines represented by a pair of coupled lines. (b) Equivalent circuit of the Mouw's hybrid junction as it is excited from port 1.

## II. Theory of Mouw's Hybrid Junction with Transmission-Line Losses

The Mouw's hybrid junction, as shown in Fig. 1(a), is a broad-band magic-T-type hybrid [1]. In Fig. 1(a), nodes $11'$ represents port 1, nodes $22'$ represents port 2, nodes $33'$ represents port 3, and nodes $44'$ represents port 4. Ports 1 and 2 are terminated with$R_{12}$ and ports 3 and 4 are terminated with $R_{34}$, respectively. This hybrid junction had been analyzed in [1] based on lossless transmission-line theory. Mouw's paper suggested that the coaxial line, waveguide, double-sided strip line, or lumped circuit transformer could realize the hybrid junction. Here, we propose a planar circuit Mouw's hybrid junction, which is realized by two CPW to CPS T-junctions. The CPS can be considered as a pair of coupled transmission lines, as shown in Fig. 1(a). Assume that the coupled lines are with the even-mode characteristic impedance of $Z_{oe}$ and the odd-mode characteristic impedance of $Z_{oo}$. The CPS characteristic impedance should be $2Z_{oo}$. If the coupled lines are with loss, the equations presented in [1] should be modified. Assume that the coupled lines are with even-mode propagation constant $\gamma_e$ and odd-mode propagation constant $\gamma_o$, respectively. When the circuit is excited from port 1, the hybrid junction can be equivalent to a circuit shown in Fig. 1(b). The terminating resistance of ports 3 and 4 are divided into two of $R_{34}/2$, respectively, for symmetry. The center points of the resistors should be RF virtually grounded. Therefore, the center point of the four $R_{34}/2$ resistors can be connected, as shown in Fig. 1(b). Suppose that all the physical lengths of

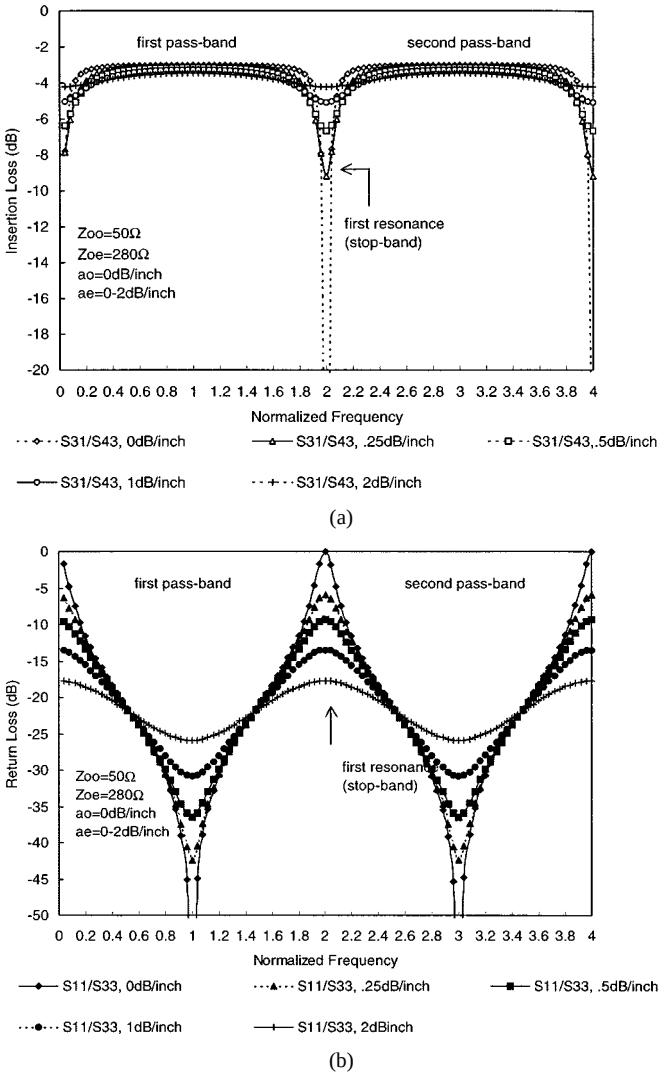


Fig. 2. Calculated performances of Mouw's hybrid junction with different $\alpha_e$ values. (a) Insertion loss. (b) Return loss.

the CPS transmission lines are equal to $l$. Using the even- and odd-mode excitation at ports 3 and port 4 and the property of reciprocity, the scattering parameters of the hybrid junction can be obtained. The 16 scattering matrix elements are given in (1)–(4), shown at the bottom of the following page, where $\gamma_{\rm i}$ is $\alpha_{\rm i} + j\beta_{\rm i}$, $i$ is $e$ or $o$, $\alpha_{\rm i}$ represents the attenuation constant, and $\beta_{\rm i}$ represents the phase constant. The cases of $R_{34} = 2R_{12}$ and $R_{34} = R_{12}$ had been discussed in [1] with the condition of $\alpha_{\rm i} = 0$. The analysis in [1] was focused on the first passband only. As the ultra-broad-band performance is concerned, the multiple numbers of passbands and stopbands should be considered. The passbands' center frequencies are defined as $\beta_o l = (2n-1)\pi/2$, and the stopbands' center frequencies are defined as $\beta_{ol} = (n-1)\pi$, where $n = 1, 2, 3\ldots$. The impedance matching condition should hold at center frequency. This implies that

$$Z_{oo} = \sqrt{\frac{R_{12}R_{34}}{2}}. \tag{5}$$

$Z_{oe}$ can be chosen arbitrarily. However, it influences bandwidth of the stopbands. Our mixer is designed with $R_{12} = 50\,\Omega$ and $R_{34} = 100\ \Omega$. Therefore, $Z_{oo}$ should be 50 $\Omega$. Fig. 2

shows the calculated responses according to different $\gamma_e$ with $Z_{oo} = 50\ \Omega$ and $Z_{oe} = 280\ \Omega$. The frequency in Fig. 2 is normalized with the center frequency of the first passband. The stopbands are located at the even multiples of the center frequency, as shown in Fig. 2. These transmission dips and reflection peaks could be explained as follows. From the equivalent circuit shown in Fig. 1(b), if the circuit is excited at port 1, the CPW-CPS T-junction at the upper left-hand side of the figure forms a dual balun. The second CPW–CPS dual balun in Fig. 1(b), at the bottom right-hand side of the figure, is just loaded to ports 3 and port 4 as a ring circuit with ring characteristic impedance of $Z_{oe}/2$. The midpoint of the ring is RF virtually grounded and the port 2 connected to this point could be removed without influencing the excitation. If the excitation is from port 2, the situation is the same as the former case, except that the phase of outgoing waves between ports 3 and 4 are in-phase in this case and out of phase in the former case. The circuit is just like a notch filter of order one when we look at Fig. 1(b). The property of the filter in Fig. 1(b) is that the higher $Z_{oe}$, the narrower the stopband. As $Z_{oe}$ and $\alpha_e$ are both high enough, the stopband can be damped out, as shown in Fig. 2. The values of $\alpha_e$ in Fig. 2 are 0.25, 0.5, 1.0, and 2.0 dB/in, respectively. When $\alpha_e$ increases to 2 dB/in, the return losses of the hybrid junction is better than 18 dB with insertion loss of 4.2 dB (it should equal to 3 dB for an ideal hybrid junction) at the center frequencies of the stopbands. This performance is good enough for ultra-broad-band mixer application. According to the (1) and (2), the return loss of ports 3 and 4 is equal to that of ports 1 and 2 only for the case of $R_{34} = 2R_{12}$. The return loss of ports 3 and 4 will not be equal to that of ports 1 and 2, especially at the stopband center frequencies if $R_{34}$ is not equal to $2R_{12}$ and $\alpha_e$ is not equal to zero.

---

$$S_{11} = S_{22} = \frac{\frac{R_{34}}{2}\left(\cosh(\gamma_o l) - \frac{R_{12}}{Z_{oo}}\sinh(\gamma_o l) + \frac{Z_{oo}}{Z_{oe}}\sinh(\gamma_o l)\coth(\gamma_e l) - \frac{R_{12}}{Z_{oe}}\cosh(\gamma_o l)\coth(\gamma_e l)\right) + Z_{oo}\sinh(\gamma_o l) - R_{12}\cosh(\gamma_o l)}{\frac{R_{34}}{2}\left(\cosh(\gamma_o l) + \frac{R_{12}}{Z_{oo}}\sinh(\gamma_o l) + \frac{Z_{oo}}{Z_{oe}}\sinh(\gamma_o l)\coth(\gamma_e l) + \frac{R_{12}}{Z_{oe}}\cosh(\gamma_o l)\coth(\gamma_e l)\right) + Z_{oo}\sinh(\gamma_o l) + R_{12}\cosh(\gamma_o l)} \tag{1}$$

$$S_{33} = S_{44} = \frac{\frac{R_{34}}{2}\left(-\cosh(\gamma_o l) - \frac{R_{12}}{Z_{oo}}\sinh(\gamma_o l) + \frac{Z_{oo}}{Z_{oe}}\sinh(\gamma_o l)\coth(\gamma_e l) - \frac{R_{12}}{Z_{oe}}\cosh(\gamma_o l)\coth(\gamma_e l)\right) + Z_{oo}\sinh(\gamma_o l) - R_{12}\cosh(\gamma_o l)}{\frac{R_{34}}{2}\left(\cosh(\gamma_o l) + \frac{R_{12}}{Z_{oo}}\sinh(\gamma_o l) + \frac{Z_{oo}}{Z_{oe}}\sinh(\gamma_o l)\coth(\gamma_e l) + \frac{R_{12}}{Z_{oe}}\cosh(\gamma_o l)\coth(\gamma_e l)\right) + Z_{oo}\sinh(\gamma_o l) + R_{12}\cosh(\gamma_o l)} \tag{2}$$

$$S_{13} = S_{31} = S_{23} = S_{32} = S_{14} = S_{41} = -S_{23} = -S_{32} = \frac{\sqrt{R_{12}R_{34}}}{\frac{R_{34}}{2}\left(\cosh(\gamma_0 l) + \frac{R_{12}}{Z_{oo}}\sinh(\gamma_o l) + \frac{Z_{oo}}{Z_{oe}}\sinh(\gamma_o l)\coth(\gamma_e l) + \frac{R_{12}}{Z_{oe}}\cosh(\gamma_o l)\coth(\gamma_e l)\right) + Z_{oo}\sinh(\gamma_o l) + R_{12}\cosh(\gamma_o l)} \tag{3}$$

$$S_{12} = S_{21} = S_{43} = S_{34} = 0 \tag{4}$$

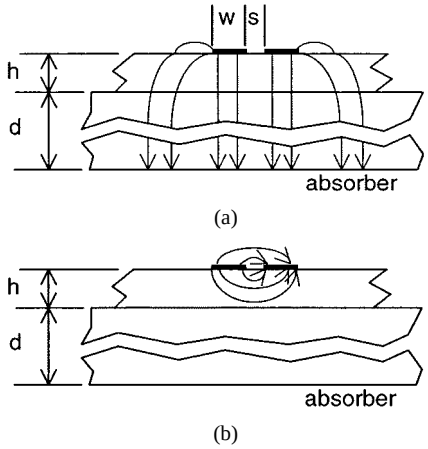


Fig. 3. Cross-sectional view and $E$-field lines of the ABCPS. (a) Even mode. (b) Odd mode (CPS mode) (substrate dielectric constant $\varepsilon = 9.8$, substrate thickness $h = 25$ mil, suspended height (absorber thickness) $d = 200$ mil).

An ABCPS, shown in Fig. 3, could realize a coupled line with 50 $\Omega$, $Z_{oo}$, very high $Z_{oe}$, very low $\alpha_o$, and very high $\alpha_e$. The cross-sectional view and $E$-field lines of an ABCPS is shown in Fig. 3. In Fig. 3, almost no $E$-field lines of the odd mode (or CPS mode) go through the absorbing material if the substrate is thick enough. However, most of the $E$-field lines of the even mode go through the absorbing material. The field penetrating into the absorber causes $\alpha_e$ much higher than $\alpha_o$. A general-purpose rubber-type absorber is used in the proposed mixer. Better performances may be obtained if it uses an absorber that is designed for absorbing microwave energy especially near the resonant frequency.

Two methods are proposed in this paper to increase the even-mode impedance. Using a very thin line and suspending the substrate much higher than the substrate thickness is the first method to achieve high even-mode impedance. Three cross-sectional structures, namely, ABCPS, SSCPS, and CBCPS, of the mixers are presented in this paper to compare their performances. The linewidths $W$ and gap widths $S$ of the CPS lines and the corresponding line parameters are listed in Table I. The values listed in Table I correspond to CBCPS and SSCPS with a suspended height that is the same as the absorber thickness. An electromagnetic (EM) simulator (Microwave Office, Applied Wave Research Inc., El Segundo, CA) is used to calculate the line parameters. The line parameters of ABCPS are not calculated because the detailed material parameters are not available. The spiral structure described in [6] is the second method to increase the input impedance of the even mode. The spiral has very little effect to the CPS mode, but it acts as a lumped-circuit spiral inductor for the even mode. The effect of this spiral CPS is equivalent to a straight CPS line with very high even-mode characteristic impedance. However, as with most of the lumped-circuit spiral inductors, the spiral CPS has the problem of self-resonance. Both of the ABCPS and spiral CPS methods for increasing the mixer bandwidth are discussed and the results are explained in the following section.

Table I is based on a 25-mil-thick $Al_2O_3$ substrate and 200-mil suspended height.

TABLE I
CPS PARAMETERS

| | Line width W (mil) | Gap spacing S (mil) | $Z_{cps}$ for SSCPS ($\Omega$) | $Z_{oe}$ for SSCPS ($\Omega$) | $Z_{cps}$ for CBCPS ($\Omega$) | $Z_{oe}$ for CBCPS ($\Omega$) |
|---|---|---|---|---|---|---|
| 1 | 5 | 4 | 100.8 | 260 | 96.2 | 103.3 |
| 2 | 4 | 3 | 98.8 | 280 | 96.2 | 116 |
| 3 | 2 | 1.8 | 101 | 320 | 101 | 148 |

## III. MIXER DESIGN AND PERFORMANCES

Three different layouts with CPS width and spacing corresponding to nos. 1–3 in Table I are realized. The CPS length $l$ in all three layouts equals 370 mil from the T-junction to diode quad (including extra 30-mil length for connecting the quad). A planar ultra-broad-band Mouw's mixer is shown in Fig. 4(a). It is the layout of the no. 3 mixer with CPS width $W = 2$ mil and spacing $S = 1.8$ mil. Fig. 4(b) is the photograph of the mixer [same as Fig. 4(a)]. The mixer diode used in the mixers is DME3178 (the new part number is DME2178) star quad from Alpha Inc., Woburn, MA. This is a $Ku$-band silicon beam-leaded Schottky diode star quad with maximal $R_s$ of 16 $\Omega$ and typical $C_j$ of 0.1 pF for each diode. The bottom right-hand-side CPW-CPS T-junction dual balun has two CPS jumps, as shown in Fig. 4(a). The left-hand-side CPS jump is required for crossing the upper left-hand-side CPW-CPS T-junction dual balun, as can be seen in Fig. 4(a). However, the right-hand-side CPS jump in Fig. 4(a) is for balancing of the electrical length of the right-hand-side CPS arm to the left-hand-side CPS arm. Each jump can be realized by a pair of bonding wire, a pair of gold ribbon, or a pair of air bridges [for monolithic microwave integrated circuits (MMICs)]. The coupling between two CPS lines through the jump wires has been studied using EM simulation. The coupling is negligible because the $E$-fields in two CPS lines are perpendicular to each other. The IF signal is picked up from center of the star quad via a CPW line at upper right-hand side of Fig. 4(a). The IF DC return is through four CPS lines and grounded at the T-junctions. These dc return paths limit the IF bandwidth because the CPS lines, which are in even-mode operation for the IF signal, become an open circuit at the diode end when $\beta_e l = \pi/2$. Therefore, the IF bandwidth of this star mixer cannot overlap the RF bandwidth. The IF signal of the lower left-hand-side mixer diode in the diode quad is grounded through one more CPS loop than the other three diodes. Theoretically, a bonding wire connects the lower left-hand-side diode and the peripheral ground plane can balance the IF grounding path. This bonding wire works as an RF choke and as an IF dc return path simultaneously. However, the measured IF performance changes very little when the mixer is with this bonding wire. The length $l$ of the CPS can be decreased to get higher IF frequency. Consequently, the RF bandwidth shrinks at the low-frequency end due to smaller CPS length. A mixer with shorter CPS length of 190 mil and with $W = 5$ mil and $S = 4$ mil is designed for comparing the RF and IF bandwidth.

The $R_{34}$ in Fig. 1(a) is chosen to be 100 $\Omega$ because it shows the best return loss of the hybrid junction near the resonant

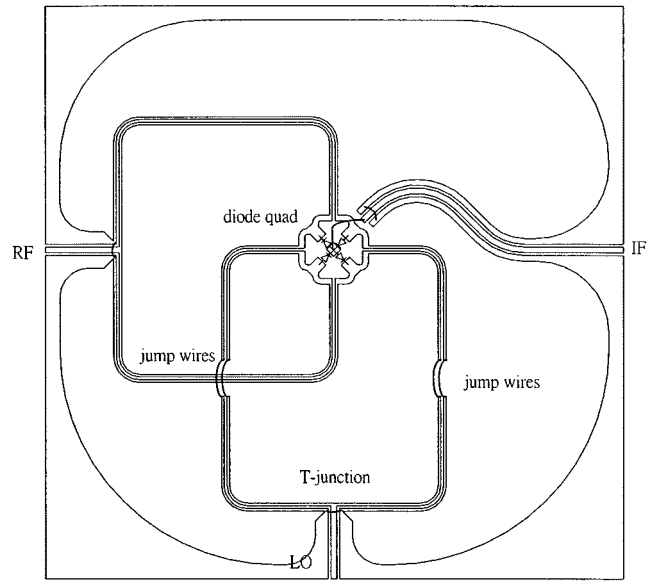


(a)

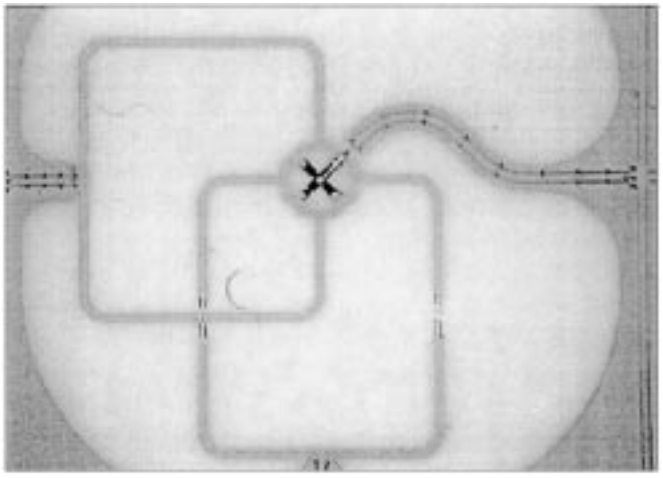

(b)

Fig. 4. (a) Layout and (b) photograph of mixer with 370-mil CPS length and with $W = 2$ mil and $S = 1.8$ mil.

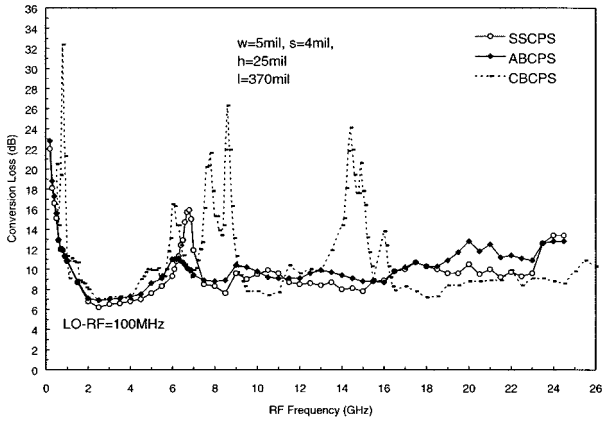


(a)

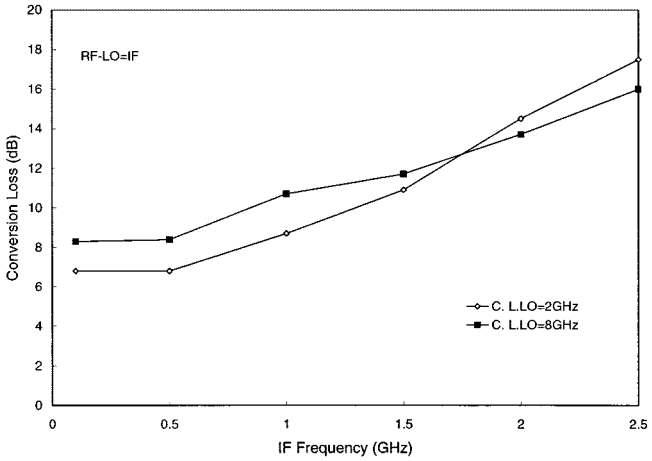


(b)

Fig. 5. Measured performances of the mixer with CPS length of 370 mil and CPS parameters corresponding to no. 1 in Table I. (a) Conversion loss versus RF frequency. (b) Conversion loss versus IF frequency.

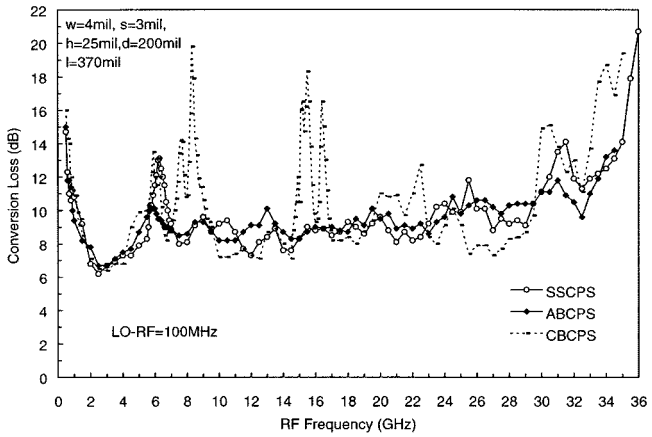


Fig. 6. Measured conversion loss of the mixer with CPS length of 370 mil and CPS parameters corresponding to no. 2 in Table I.

frequencies under a high $\alpha_e$ situation. As each diode in the diode quad has the equivalent RF resistance of 50 Ω, the hybrid junction will meet the condition of $R_{34} = 100\ \Omega$. Usually, the equivalent RF resistance of a Schottky diode is approximately inversely proportion to the LO power level. Therefore, the impedance matching condition of $R_{34} = 100\,\Omega$ can be met if the diodes are properly pumped.

Figs. 5–7 show the measured performances of the mixer with CPS length of 370 mil and CPS parameters corresponding to nos. 1–3 in Table I, respectively. A mixer with shorter CPS length of 190 mil and CPS width of 5 mil and spacing of 4 mil is measured for comparing of the IF/RF performances. Figs. 5 and 8 depict two mixers, which are to be compared (the only difference being their CPS length). The measured results are described as follows. The IF 10-dB conversion-loss bandwidth is dc to 0.75 GHz for the mixer with 370-mil CPS length and dc to 1.8 GHz for the mixer with 190-mil CPS length. The RF 10-dB conversion-loss bandwidth starts from 1.3 GHz for the mixer with 370-mil CPS length and stars from 2.5 GHz for the mixer with 190-mil CPS length. The first resonance occurs at about 6.7 GHz for the mixer with 370-mil CPS length and 13.7 GHz for the mixer with 190-mil CPS length. The first resonance is occurred at the frequency of even-mode CPS length equals to half wavelength $(\lambda/2)$. Higher order resonance can only be found in the CBCPS mixer due to much lower even-mode characteristic

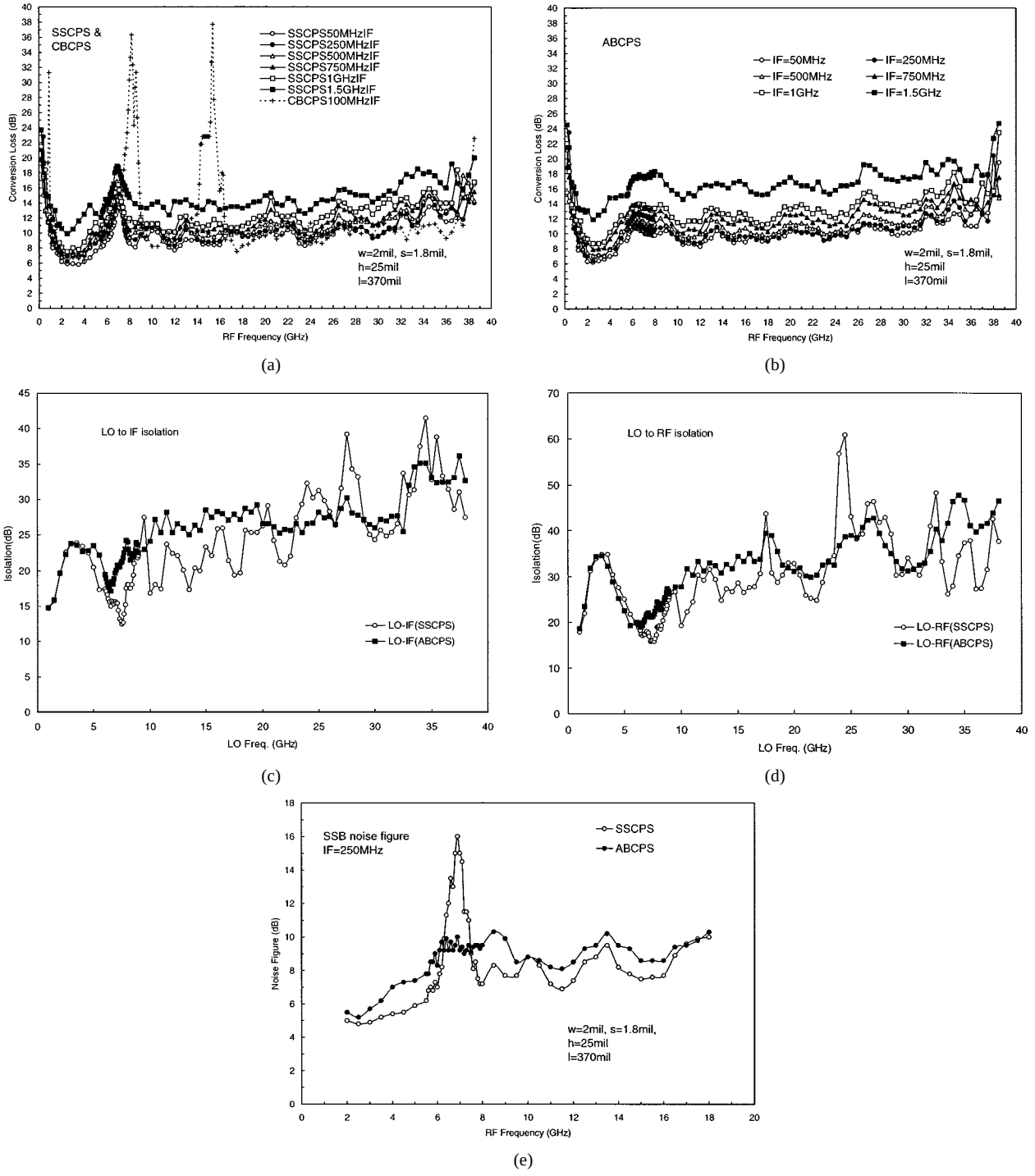


Fig. 7. Measured performances of the mixer with CPS length of 370 mil and CPS parameters corresponding to no. 3 in Table I. (a) Conversion loss of SSCPS and CBCPS mixer under various IF frequencies. (b) Conversion loss of ABCPS mixer under various IF frequencies. (c) LO to IF isolation of the SSCPS and ABCPS mixer. (d) LO to RF isolation of the SSCPS and ABCPS mixer. (e) SSB noise figure of the SSCPS and ABCPS mixer.

impedance comparing to that of the SSCPS mixer. The conversion loss peaks of the ABCPS mixers improve to about 10 dB near the resonance frequency, as was expected. The conversion loss of the mixer with no. 3 CPS parameters in Table I are measured under various IF frequencies, as shown in Fig. 7(a) and (b). The conversion loss degrades gradually as the IF frequency increases. The first resonant frequencies of all three types of the mixers, namely, ABCPS, SSCPS, and CBCPS, are very close. It can also be seen from the figures that the CBCPS mixer has the widest stopband bandwidth due to its much lower even-mode impedance. The RF bandwidths of mixers with CPS length of 370 mil are described as follows. The RF bandwidth is from 0.9 to 19.5 GHz with conversion loss less than 11.5 dB for the no. 1 ABCPS mixer, and it is from 0.9 to 29.9 GHz with conversion loss less than 10.5 dB for the no. 2 ABCPS mixer. The RF bandwidth of the no. 3 ABCPS mixer is from 0.9 to 31.5 GHz with conversion loss less than 10.8 dB. The RF bandwidth of the ABCPS mixer with 190-mil CPS length and with $W = 5$ mil

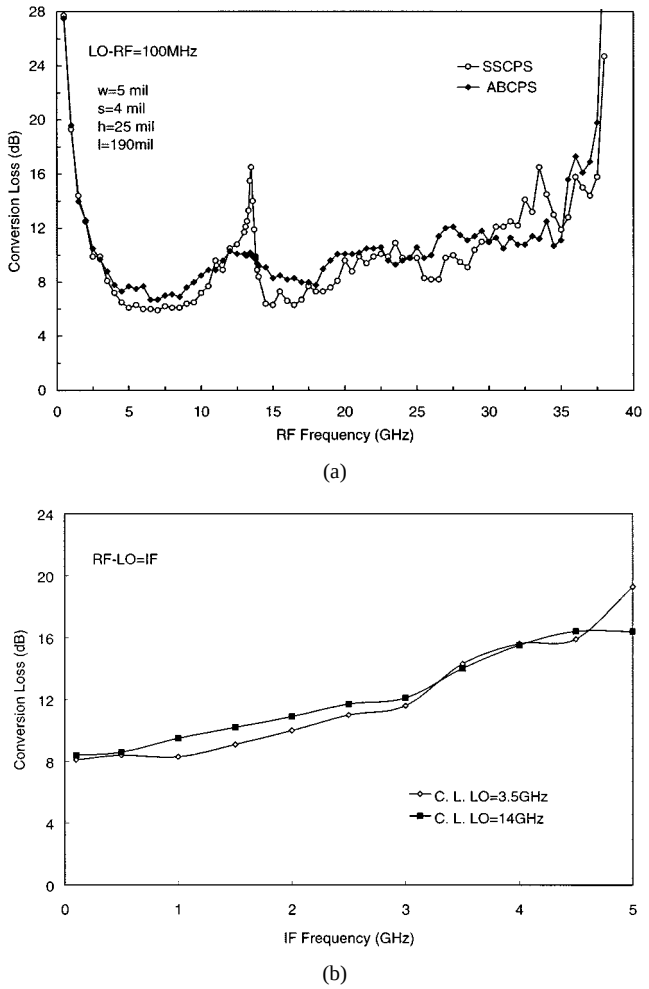


Fig. 8. Measured performances of the mixer with same CPS parameters in Fig. 5, but shorter CPS length of 190 mil. (a) Conversion loss versus RF frequency. (b) Conversion loss versus IF frequency.

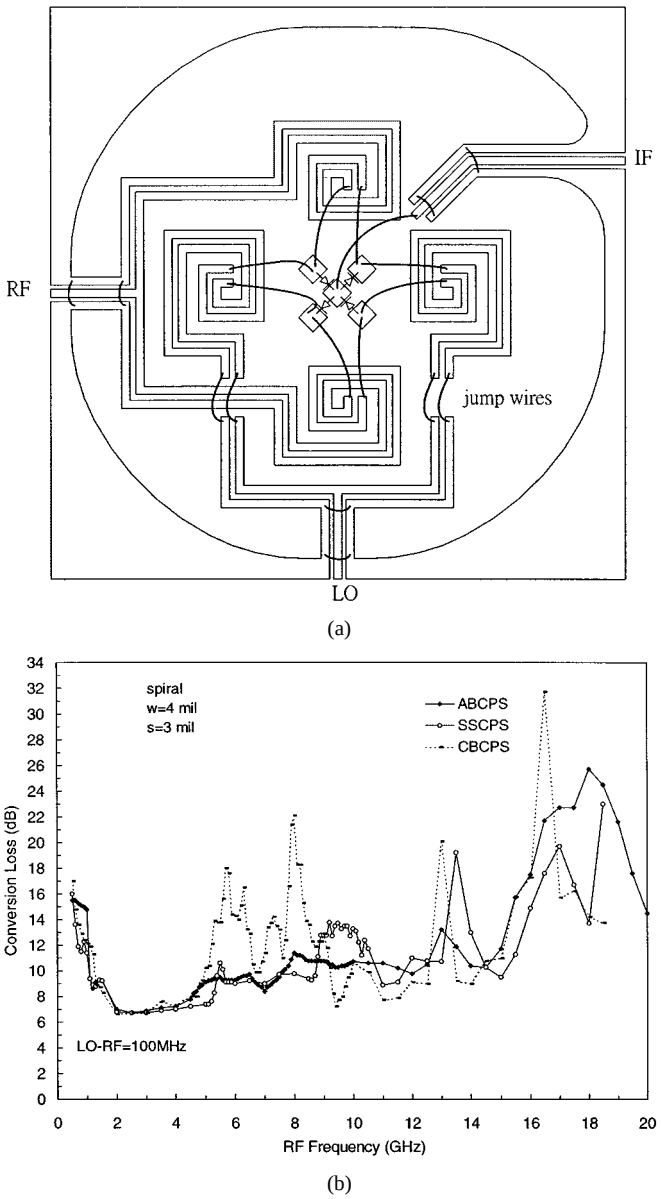


Fig. 9. Layout and measured conversion loss of the spiral CPS star mixer with CPS parameters the same as in Fig. 6. (a) Mixer layout. (b) Measured conversion loss.

and $S = 4$ mil is from 2.5 to 33.5 GHz with conversion loss less than 11 dB. The conversion loss, which degrades gradually from low to high frequency, is mainly due to the performance degradation of the mixer diodes. A GaAs diode quad with a higher diode cutoff frequency may be required to reach higher frequencies. The diode quad used in this paper, however, is a commercially available star quad with the highest cutoff frequency. The measured LO to IF and LO to RF isolation of the no. 3 SSCPS mixer and ABCPS mixer are shown in Fig. 7(c) and (d). The isolation is also degraded at the stopband frequencies. However, the isolation of the ABCPS mixer is better than that of SSCPS mixer at the stopband frequencies. The penalties of using an absorber to damp out the resonance are the degradation of the conversion loss and noise figure over the entire bandwidth, except the stopband. The degradation of the conversion loss is typically from 0.5 to 1 dB, as can be seen in the conversion-loss curves. The measured singel-sideband (SSB) noise figure of the no. 3 SSCPS and ABCPS mixer is shown in Fig. 7(e). The noise figure improves a lot near the resonance frequency, but degrades typically about 1 dB at other frequencies. The CBCPS mixers show strong resonance phenomenon due to relatively low even-mode impedance. The higher order resonant peaks of CBCPS mixers are not damped out, as can be seen in the conversion loss curves. Moreover, the absorber underneath the substrate of the CBCPS mixer is useless to damp these resonant peaks out due to the ground plane between the substrate and absorber. Therefore, CBCPS mixers can only be used in their passbands, especially the first passband.

As mentioned in the previous section, a spiral CPS may increases the even-mode input impedance at the diode end. A mixer with spiral CPS layout and with CPS parameters of $W = 4$ mil and $S = 3$, as shown in Fig. 9(a), is realized to study the effect of spiral design. The measured conversion loss of this spiral CBCPS mixer is shown in Fig. 9(b). However, the mixer is not an ultra-broad-band mixer, as can be seen in Fig. 9(b). This is due to the self-resonance of the CPS spiral inductor. Nevertheless, in the case of a CBCPS mixer, this spiral layout should be much more broad band than the straight layout, as predicted in [6]. A 3-dB conversion-loss passband is defined to compare

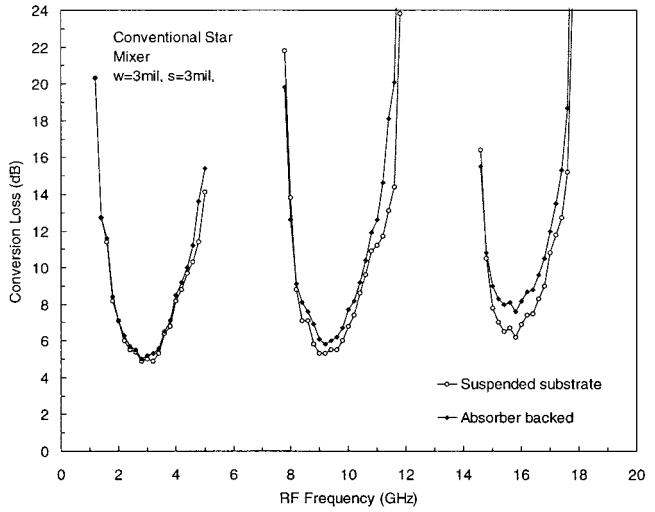


Fig. 10. Measured conversion loss of a conventional FCPW star mixer.

the bandwidth between mixers in this paper. The 3-dB conversion-loss passband is defined as a frequency band between two corner frequencies, in which the conversion losses at these two corner frequencies are 3 dB worse than that of center frequency. The 3-dB conversion loss passband of the spiral CBCPS mixer is from 1.25 to 4.95 GHz in the first passband, which corresponds to a relative bandwidth of 119%. The 3-dB conversion-loss passband of the straight CBCPS mixer is from 2.3 to 5.8 GHz, as shown in Fig. 6(a). The relative bandwidth of the straight CBCPS mixer is 86%. Indeed, the spiral design increases the first passband a lot. The spiral CBCPS is a good choice for the MMIC mixer design because the SSCPS and ABCPS are both not usable in MMICs.

## IV. Discussions

According to original Mouw's theory, many different kinds of transmission lines can realize the Mouw's hybrid junction. A finite-ground-width coplanar waveguide (FCPW) is also a good choice to realize the planar circuit Mouw's hybrid junction. The hybrid junction theory developed in Section II is still valid in the FCPW case, except $Z_{oo}$ in (1)-(3) should equal $Z_{\mathrm{cpw}}/2$. An FCPW–FCPW T-junction type mixer has been fabricated, and the measured performance (not shown in this paper) is not as good as a CPW–CPS T-junction type mixer. The relative 3-dB bandwidth of the suspended substrate FCPW (SSFCPW) mixer is 93.4%, which is less than that of the SSCPS mixer (it is 124% in Fig. 6). Besides, the absorber-backed finite-ground-width coplanar waveguide (ABFCPW) mixer shows serious performance degradation in the passbands. The reasons are that the even-mode (suspended-stripline-like mode) characteristic impedance of a 100-$\Omega$ FCPW line cannot be made high and the odd-mode (CPW mode) electric field of the 100-$\Omega$ FCPW goes partially through the absorber because the total width of the 100-$\Omega$ FCPW is very large. Another issue for the star mixer is the difference of RF performance between the conventional star mixer described in [2]–[4] and the mixer proposed in this paper. Authors have realized an FCPW conventional-type Marchand dual-balun star mixer [3] to see the behavior of passbands and stopbands. The measured conversion loss of these conventional SSFCPW and ABFCPW star mixers is shown in Fig. 10. The conversion-loss behavior of this conventional star mixer is summarized as follows. The first 3-dB passband of this conventional star mixer is from 2 to 3.8 GHz, which corresponds to a relative bandwidth of 62%. The first stopband with conversion loss worse than 15 dB is from 5 to 8 GHz. The stopband and passband performances of the ABCPW mixer are almost the same as that of the SSCPW mixer, as can be seen in Fig. 10. The passbands and stopbands of the conventional star mixer appear periodically. Unlike this newly proposed Mouw's star mixer, the absorbing material cannot damp out the stopbands of the conventional star mixer. This means that the conventional star mixer cannot be used as an ultra-broad-band mixer. The Mouw's hybrid junction is very useful in realization of an ultra-broad-band star mixer. Moreover, it can also be used to realize a triply balanced mixer if a double-ring diode quad and an extra IF balun are used. In fact, a triply balanced mixer that is realized by Mouw's hybrid junction faces the same even-mode resonance problem. The methods to solve an even-mode resonance problem, which is developed in this paper, are also valid in triply balanced mixer.

## V. Conclusions

The ultra-broad-band star mixer using CPW-CPS planar Mouw's hybrid junction has been developed. The theory of the elimination of the even-mode resonance has been developed. Theoretically, a coupled transmission line with a lossy even mode can damp out the resonance. The absorber-backed CPS can damp out the resonance effectively. The penalties of using an absorber to damp out the resonance are typically from 0.5- to 1-dB degradation of the conversion loss and noise figure. Higher even-mode impedance causes broader first passband bandwidth. In case of a CBCPS, the even-mode resonance cannot be damped out. The CBCPS mixer with a spiral CPS layout has also been developed for increasing the first passband bandwidth. The first passband bandwidth of this spiral CPS mixer, approximately 4 : 1 bandwidth, was much broader than that of a straight CPS mixer.

## Acknowledgment

The authors wish to thank C. S. Wu, Chung-Shan Institute of Science and Technology, Lung-Tang, Taiwan, R.O.C., for his constant support and valuable suggestions.

## References

[1] R. B. Mouw, "A broad-band hybrid junction and application to the star modulator," *IEEE Trans. Microwave Theory Tech.*, vol. MTT-16, pp. 154–161, Nov. 1968.

[2] B. R. Hallford, "A designer's guide to planar mixer baluns," *Microwaves*, pp. 52–57, Dec. 1979.

[3] S. A. Maas, "A broad-band, planar, doubly balanced monolithic $Ka$-band diode mixer," *IEEE Trans. Microwave Theory Tech.*, vol. 41, pp. 2330–2335, Dec. 1993.

[4] Y. I. Ryu, K. W. Kobayashi, and A. K. Oki, "A monolithic broad-band doubly balanced EHF HBT star mixer with novel microstrip baluns," in *IEEE Microwave Millimeter-Wave Monolithic Circuit Symp. Dig.*, 1995, pp. 155–158.

[5] N. Marchand, "Transmission line conversion transformers," *Electronics*, vol. 17, no. 12, pp. 142–145, Dec. 1942.
[6] S. Maas, M. Kintis, F. Fong, and M. Tan, "A broadband planar monolithic ring mixer," in *Microwave Millimeter Wave Monolithic Circuit Symp. Dig.*, 1996, pp. 51–54.

**Chi-Yang Chang** (S'88–M'95) was born in Taipei, Taiwan, R.O.C., on December 20, 1954. He received the B.S. degree in physics and the M.S. degree in electrical engineering from the National Taiwan University, Taiwan, R.O.C., in 1977 and 1982, respectively, and the Ph.D. degree in electrical engineering from The University of Texas at Austin, in 1990..

From 1979 to 1980, he was a Teaching Assistant with the Department of Physics, National Taiwan University. From 1982 to 1988, he was an Assistant Researcher with the Chung-Shan Institute of Science and Technology (CSIST), where he was in charge of development of microwave integrated circuits (MICs), microwave subsystems, and millimeter-wave waveguide $E$-plane circuits. He returned to CSIST, where from 1990 to 1995, he was an Associate Researcher in charge of development of uniplanar circuits, ultra-broad-band circuits, and millimeter-wave planar circuits. In 1995, he joined the faculty of the Department of Communication Engineering, National Chiao-Tung University, Hsinchu, Taiwan, R.O.C., where he is currently an Associate Professor. His research interests include microwave and millimeter-wave passive and active circuit design, planar miniaturized filter design, and MMIC design.

**Ching-Wen Tang** was born in Nantou, Taiwan, R.O.C., on July 16, 1968. He received the B.S. degree in electronic engineering from the Chung Yuan Christian University, Chungli, Taiwan, R.O.C., in 1991, the M.S. degree in communication engineering from the National Chiao-Tung University, Hsinchu, Taiwan, R.O.C., in 1996, and is currently working toward the Ph.D. degree at the National Chiao-Tung University.

In 1997, he joined the RF Communication Systems Technology Department, Computer and Communication Laboratories, Industrial Technology Research Institute (ITRI), Hsinchu, Taiwan, R.O.C., as a RF Engineer, where he currently develops RF passive components. His research interests include microwave and millimeter-wave mixer design, and the analysis and design of thin-film passive components.

**Dow-Chih Niu** was born in Taipei, Taiwan, R.O.C., on August 28, 1956. He received the B.S. degree in electrophysics and the M.S. degree in electronics engineering from the National Chiao-Tung University, Hsinchu, Taiwan, R.O.C., in 1978 and 1982, respectively.

From 1982 to 1991, he was with the Chung-Shan Institute of Science and Technology (CSIST), Lung-Tang, Taiwan. From 1991 to 1993, he was with the University of California at Los Angeles. He is currently with CSIST, where he is in charge of the development of microwave and millimeter-wave circuits and subsystems.